

Right Ventricular–Pulmonary Arterial Coupling in Secondary Tricuspid Regurgitation



Federico Fortuni, MD^{a,b,1}, Steele C. Butcher, MD^{a,c,1}, Marlieke F. Dietz, MD^a, Pieter van der Bijl, MDPH^a, Edgard A. Prihadi, MD^a, Gaetano M. De Ferrari, MD^b, Nina Ajmone Marsan, MD, PhD^a, Jeroen J. Bax, MD, PhD^a, and Victoria Delgado, MD, PhD^{a,*}

Chronic pressure-overload induces right ventricular (RV) adaptation to maintain RV–pulmonary arterial (PA) coupling. RV remodeling is frequently associated with secondary tricuspid regurgitation (TR) which may accelerate uncoupling. Our aim is to determine whether the non-invasive analysis of RV–PA coupling could improve risk stratification in patients with secondary TR. A total of 1,149 patients (median age 72[IQR, 63 to 79] years, 51% men) with moderate or severe secondary TR were included. RV–PA coupling was estimated using the ratio between two standard echocardiographic measurements: tricuspid annular plane systolic excursion (TAPSE) and pulmonary artery systolic pressure (PASP). The risk of all-cause mortality across different values of TAPSE/PASP was analyzed with a spline analysis. The cut-off value of TAPSE/PASP to identify RV–PA uncoupling was based on the spline curve analysis. At the time of significant secondary TR diagnosis the median TAPSE/PASP was 0.35 (IQR, 0.25 to 0.49) mm/mm Hg. A total of 470 patients (41%) demonstrated RV–PA uncoupling (<0.31 mm/mm Hg). Patients with RV–PA uncoupling presented more frequently with heart failure symptoms had larger RV and left ventricular dimensions, and more severe TR compared to those with RV–PA coupling. During a median follow-up of 51 (IQR, 17 to 86) months, 586 patients (51%) died. The cumulative 5-year survival rate was lower in patients with RV–PA uncoupling compared to their counterparts (37% vs 64%, $p < 0.001$). After correcting for potential confounders, RV–PA uncoupling was the only echocardiographic parameter independently associated with all-cause mortality (HR 1.462; 95% CI 1.192 to 1.793; $p < 0.001$). In conclusion, RV–PA uncoupling in patients with secondary TR is independently associated with poor prognosis and may improve risk stratification. © 2021 The Author(s). Published by Elsevier Inc. This is an open access article under the CC BY license (<http://creativecommons.org/licenses/by/4.0/>) (Am J Cardiol 2021;148:138–145)

Significant (moderate or severe) tricuspid regurgitation (TR) is associated with increased morbidity and mortality.^{1–3} Secondary TR is the predominant mechanism of TR and is frequently due to left-sided valvular heart disease and left ventricular diastolic or systolic dysfunction.^{4–6} These conditions commonly result in elevated pulmonary pressures and increased right ventricular (RV) afterload, with the RV adapting to the increased load through hypertrophy and/or dilation.⁷ RV dilation is accompanied by progressive tricuspid annular dilation and papillary muscle displacement, key factors in the development of secondary TR. Quantification of RV–pulmonary arterial (PA) coupling may provide important insights into the mechanism of adaptation of RV

contractility to afterload in patients with secondary TR. The ratio between RV end-systolic elastance (Ees) and pulmonary arterial elastance (Ea) estimated from invasive pressure–volume loops is the reference standard.⁷ Recently, the ratio between tricuspid annular plane systolic excursion (TAPSE) and pulmonary artery systolic pressure (PASP) measured on echocardiography has shown a good correlation with invasively estimated RV–PA coupling.⁸ A reduced TAPSE/PASP ratio suggests that RV contractility is uncoupled from its load and portends a poor prognosis in patients with pulmonary hypertension.⁹ The aim of the present study is to determine whether the noninvasive analysis of RV–PA coupling with the use of the TAPSE/PASP ratio could improve risk stratification in patients with significant secondary TR.

^aDepartment of Cardiology, Leiden University Medical Center, Leiden, The Netherlands; ^bDivision of Cardiology, Department of Medical Sciences, AOU Città della Salute e della Scienza, University of Turin, Turin, Italy; and ^cDepartment of Cardiology, Royal Perth Hospital, Perth, Western Australia, Australia. Manuscript received January 1, 2021; revised manuscript received and accepted February 19, 2021.

This work was funded by an unrestricted research grant from Edwards Lifesciences (HSUSTHV2018017).

¹These authors contributed equally to this work.

See page 144 for disclosure information.

*Corresponding author: Tel: (3171) 526-2020; fax: (3171) 526-6809.

E-mail address: v.delgado@lumc.nl (V. Delgado).

Methods

A query of the echocardiographic database of the Leiden University Medical Center (Leiden, The Netherlands) was performed to identify patients diagnosed with moderate or severe secondary TR between June 1995 and September 2016. Patients with primary TR (due to valve prolapse, endocarditis, rheumatic or carcinoid heart disease), congenital heart disease, and those who underwent tricuspid valve

interventions after the diagnosis of significant TR were excluded. In addition, patients with incomplete data to assess RV–PA coupling (i.e., TAPSE and/or PASP) were specifically excluded. Clinical and demographic data at the time of the diagnosis of significant secondary TR were collected from the departmental Cardiology Information System (EPD-VisionVR; Leiden University Medical Centre, Leiden, The Netherlands). This retrospective analysis of clinically acquired data was approved by the institutional review board of the Leiden University Medical Centre that waived the need for patient written informed consent.

Clinical characteristics included cardiovascular risk factors, comorbidities, New York Heart Association (NYHA) functional class, medical therapy, and the presence of cardiac devices. Transthoracic echocardiographic data were acquired with patients at rest in the left lateral decubitus position using available ultrasound systems (Vivid 7, E9, and E95 systems; GE-Vingmed) equipped with 3.5 MHz or M5S transducers. Data were stored digitally in a cine-loop format for offline analysis with the EchoPac software (EchoPac version 203 and 204, GE-Vingmed). The digitized echocardiographic data were retrospectively reanalyzed taking into account current guidelines and therefore, the present study does not simply concern tabulation of descriptive data included in the clinical reports. RV dimensions were measured on an RV-focused apical view and included end-diastolic basal and mid diameter, end-diastolic base-to-apex length, end-diastolic, and end-systolic areas.¹⁰ RV systolic function was estimated based on TAPSE measured on M-mode recordings of the lateral tricuspid annulus. RV fractional area change was also calculated with the following formula: $(\text{end-diastolic area} - \text{end-systolic area})/\text{end-diastolic area} \times 100$. TR grade was assessed by a multiparametric approach, including qualitative, semi-quantitative, and quantitative parameters.¹¹ PASP was estimated from the TR jet peak velocity applying the simplified Bernoulli equation and adding mean right atrial pressure.¹⁰ Mean right atrial pressure was derived based on the inferior vena cava diameter and collapsibility during inspiration.¹⁰ Left ventricular ejection fraction (LVEF) was calculated using the biplane Simpson method.¹² RV–PA coupling was estimated non-invasively using the ratio between two standard echocardiographic measurements: TAPSE and PASP. TAPSE/PASP ratio is a surrogate for Ees/Ea, based on the assumption that TAPSE provides an estimate of RV contractility and PASP an estimate of RV afterload.^{8,13–14} Moreover, it was recently demonstrated that TAPSE/PASP is the only echocardiographic index that is independently associated with the gold standard invasive measurement of RV–PA coupling (i.e., Ees/Ea).⁸

The primary endpoint of this study was all-cause mortality. All patients were followed-up for the occurrence of the primary endpoint. Survival data were collected from the departmental Cardiology Information System and the Social Security Death Index.

The statistical analyses were performed using the SPSS version 25.0 (SPSS Inc, IBM Corp) and in R environment 3.6.4 (R Foundation for Statistical Computing). Categorical variables are expressed as numbers and percentages. For continuous variables, adherence to a normal distribution

was verified through visual assessment, comparing a histogram of the sample data to a normal probability curve. Normally distributed continuous variables are presented as mean \pm standard deviation while variables that are non-normally distributed are presented as median and interquartile range. To assess the hazard ratio (HR) change for all-cause mortality across a range of TAPSE/PASP values at baseline a spline curve analysis was performed. The cut-off value of TAPSE/PASP to define RV–PA uncoupling was chosen based on mortality excess and previously published data.⁸ Differences between RV–PA coupling versus uncoupling were analyzed using the unpaired Student t-test for normally distributed continuous variables, the Mann–Whitney U test for non-normally distributed continuous variables and the Pearson's chi-square test for categorical variables. The 1- and 5-year cumulative survival rates were estimated with Kaplan–Meier curves and differences between groups were analyzed using the Mantel–Cox log-rank test. A multivariable Cox proportional hazard regression analysis was conducted to assess the clinical and echocardiographic features that were independently associated with all-cause mortality. Possible confounders with a p value < 0.05 at the univariable analysis were included in the multivariable Cox regression analysis. HRs and 95% confidence intervals (CIs) were calculated. Two-sided p values < 0.05 were considered statistically significant.

Results

A total of 1,149 patients with a median age of 72 (interquartile range, 63 to 79) years fulfilled the study inclusion criteria (Supplementary Figure 1). Of these, 909 (79%) had moderate TR and 240 (21%) had severe TR. To investigate the relationship between TAPSE/PASP ratio and all-cause mortality, a spline curve analysis was performed (Figure 1). After an initial slow rise of HR, there was an increase in the HR of all-cause mortality for reduced values of TAPSE/PASP ratio (< 0.31 mm/mm Hg). Based on this analysis and previously published data,⁸ a TAPSE/PASP value < 0.31 mm/mm Hg was used to define RV–PA uncoupling and to dichotomize the population. RV–PA uncoupling at the time of significant secondary TR diagnosis was present in 470 patients (41%). When compared to patients with RV–PA coupling, those with RV–PA uncoupling were more frequently men, had a higher prevalence of cardiovascular risk factors and coronary artery disease, worse renal function, were more symptomatic (heart failure symptoms and peripheral edema), and used diuretics more frequently (Table 1). Patients with RV–PA uncoupling had significantly larger left ventricular and RV dimensions, lower LVEF, larger left atrial (LA) volumes, and more frequently had significant mitral regurgitation than those without RV–PA uncoupling (Table 2). Interestingly, those with RV–PA uncoupling had larger tricuspid regurgitant volume and vena contracta width when compared to those with RV–PA coupling.

During a median follow-up of 51 (interquartile range, 17 to 86) months, 586 patients (51%) died. Kaplan–Meier analysis demonstrated significantly reduced survival in patients with RV–PA uncoupling at 1-year (59% vs 82%, log-rank chi-square = 62.379, $p < 0.001$) and 5-year follow-up (37% vs 64%, log-rank chi-square = 86.247, $p < 0.001$;

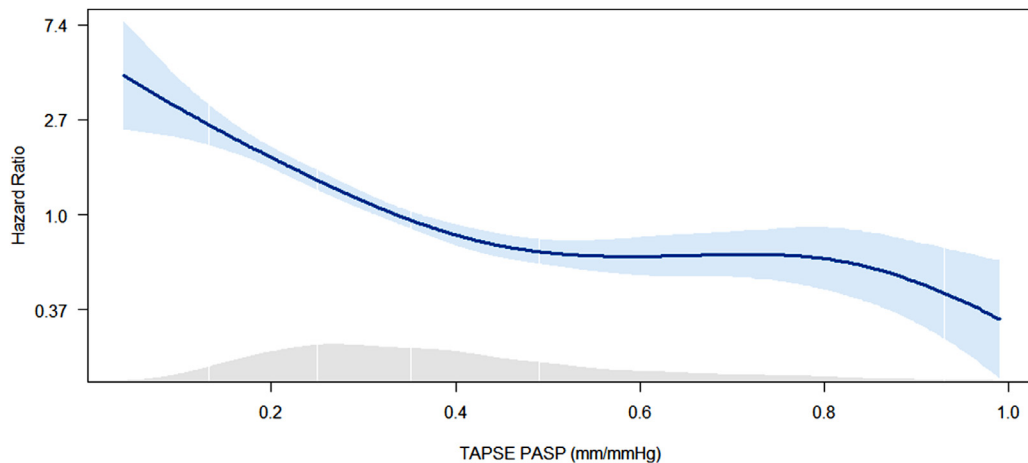


Figure 1. Spline curve for all-cause mortality according to TAPSE/PASP ratio. The curve represents the hazard ratio change for all-cause mortality with overlaid 95% confidence intervals (light-blue) across a range of TAPSE/PASP ratio at the time of significant secondary TR diagnosis. The grey density plot shows the distribution of the study population according to values of TAPSE/PASP.

TAPSE/PASP = Tricuspid annular plane systolic excursion / pulmonary artery systolic pressure ratio; TR = Tricuspid regurgitation

Figure 2). To further investigate the association between the TAPSE/PASP ratio and all-cause mortality, univariable and multivariable Cox proportional hazards models were constructed (Table 3). TAPSE/PASP was introduced as a categorical variable, utilizing the threshold derived from the spline curve analysis (0.31 mm/mm Hg). Univariable Cox regression analysis demonstrated a significant association between the following parameters and the risk of all-cause mortality: age, male gender, diabetes mellitus, known coronary artery disease, chronic obstructive pulmonary disease, renal function, heart failure symptoms, diuretic use, left ventricular systolic function, LA volume, significant left-sided valvular heart disease, RV dimensions and systolic function, PASP, individual parameters of TR severity, and RV-PA uncoupling (i.e., TAPSE/PASP < 0.31). On multivariable Cox regression analysis, RV-PA uncoupling (i.e., TAPSE/PASP < 0.31) was the only

echocardiographic parameter that retained an independent association with all-cause mortality (HR 1.46; 95% CI 1.19 to 1.79; $p < 0.001$). As shown in Figure 3, the incremental prognostic value of the TAPSE/PASP ratio and RV-PA uncoupling (i.e., TAPSE/PASP < 0.31 mm/mm Hg) was evaluated by adding these parameters to a baseline model. The addition of TAPSE/PASP ratio as a continuous variable improved the predictivity of the model compared to the addition of standard echocardiographic parameters of RV systolic function (i.e., TAPSE or fractional area change). Moreover, the addition of RV-PA uncoupling (i.e., TAPSE/PASP < 0.31 mm/mm Hg) to the same basal model yielded a higher increase in predictivity compared to the addition of RV systolic dysfunction either evaluated with TAPSE (< 17 mm) or fractional area change (<35%) using the cut-off values recommended by current guidelines¹⁵ (Figure 3).

Table 1.
Clinical and demographic characteristics

Variable	Overall (n = 1,149)	RV-PA coupling (TAPSE/PASP \geq 0.31) (n = 679)	RV-PA uncoupling (TAPSE/PASP < 0.31) (n = 470)	p value
Age (years)	72 (63-79)	72 (62 to 78)	72 (63 to 79)	0.271
Men	582 (51%)	317 (47%)	265 (56%)	0.001
Body mass index (kg/m ²)	26 \pm 4	26 \pm 4	25 \pm 4	0.489
Hypertension	854 (81%)	497 (80%)	357 (83%)	0.312
Hypercholesterolemia	501 (48%)	266 (43%)	235 (55%)	<0.001
Diabetes mellitus	208 (20%)	82 (13%)	126 (29%)	<0.001
Coronary artery disease	457 (40%)	221 (33%)	236 (51%)	<0.001
Chronic obstructive pulmonary disease	154 (15%)	84 (14%)	70 (16%)	0.258
Glomerular filtration rate (ml/min/1.73 m ²)	65 \pm 29	68 \pm 28	59 \pm 28	<0.001
Current or former smoker	319 (31%)	192 (31%)	127 (30%)	0.584
Atrial fibrillation	539 (50%)	314 (49%)	225 (51%)	0.692
New York Heart Association functional class III-IV	464 (44%)	220 (36%)	244 (56%)	<0.001
Peripheral edema	249 (23%)	109 (17%)	140 (31%)	<0.001
Diuretic use	645 (58%)	329 (50%)	316 (69%)	<0.001

PA = pulmonary arterial; PASP = pulmonary arterial systolic pressure; RV = right ventricle; TAPSE = tricuspid annular plane systolic excursion. Values are presented as mean \pm SD, median (IQR) or n (%). Percentages are calculated based on data availability.

Table 2.
Echocardiographic characteristics

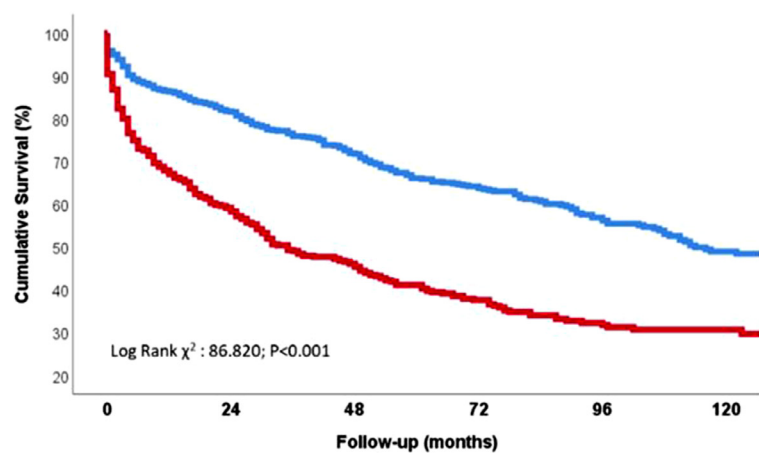
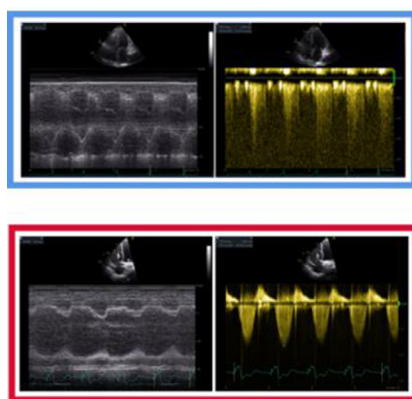
Variable	Overall (n = 1,149)	RV–PA coupling (TAPSE/PASP \geq 0.31) (n=679)	RV–PA uncoupling (TAPSE/PASP < 0.31) (n=470)	p value
Left-sided heart				
Left ventricular end-diastolic diameter (mm)	48 \pm 11	47 \pm 11	50 \pm 12	<0.001
Left ventricular end-systolic diameter (mm)	39 \pm 13	37 \pm 13	41 \pm 14	<0.001
Left ventricular end-diastolic volume (ml)	113 (80-167)	105 (80-154)	125 (82-190)	<0.001
Left ventricular ejection fraction (%)	44 \pm 16	46 \pm 15	41 \pm 16	<0.001
Left atrial maximum volume (ml)	92 (59-127)	80 (56-119)	104 (70-137)	<0.001
Significant aortic stenosis	263 (24%)	145 (22%)	118 (26%)	0.106
Significant mitral regurgitation	304 (27%)	155 (23%)	149 (32%)	0.001
Right-sided heart				
RV basal diameter (mm)	45 \pm 8	45 \pm 9	46 \pm 8	0.409
RV mid diameter (mm)	35 \pm 9	34 \pm 9	36 \pm 9	0.001
RV longitudinal diameter (mm)	72 \pm 12	71 \pm 13	74 \pm 12	<0.001
RV end-diastolic area (cm ²)	25 \pm 12	25 \pm 14	26 \pm 9	0.025
Right atrial area (cm ²)	28 \pm 11	27 \pm 11	28 \pm 10	0.078
Fractional area change (%)	34 \pm 13	36 \pm 14	31 \pm 12	<0.001
Tricuspid annular plane systolic excursion (mm)	15 \pm 5	18 \pm 5	12 \pm 3	<0.001
PASP (mm Hg)	44 \pm 16	37 \pm 11	55 \pm 15	<0.001
Tricuspid valve				
Tricuspid annulus diameter (mm)	42 \pm 8	42 \pm 8	42 \pm 8	0.106
Vena contracta (mm)	11 \pm 4	10 \pm 4	11 \pm 4	0.023
Effective regurgitant orifice area (mm ²)	68 (43-105)	68 (41-110)	68 (46-101)	0.905
Regurgitant volume (ml/beat)	65 (39-104)	59 (35-102)	73 (46-106)	<0.001
Pacemaker/Implantable cardioverter defibrillator lead	413 (37%)	245 (37%)	168 (36%)	0.887

PA = pulmonary arterial; PASP = pulmonary artery systolic pressure; RV = right ventricle; TAPSE = tricuspid annular plane systolic excursion. Values are presented as mean \pm SD, median (IQR) or n (%). Percentages are calculated based on data availability.

Discussion

In patients with moderate or severe secondary TR, the assessment of RV–PA coupling by TAPSE/PASP ratio is superior for risk stratification compared to the evaluation of conventional indices of RV systolic function such as

fractional area change or TAPSE. Interestingly, in this large cohort of patients with moderate and severe secondary TR, 41% presented with RV–PA uncoupling at the time of significant TR diagnosis, potentially indicating advanced disease and late diagnosis.



— TAPSE/PASP \geq 0.31 mm/mmHg	679	546	433	280	162	94
— TAPSE/PASP < 0.31 mm/mmHg	470	273	194	116	65	33

Figure 2. Kaplan–Meier curves for all-cause mortality. The Kaplan–Meier curves demonstrate the higher survival rates of patients with RV–PA coupling (TAPSE/PASP ratio: \geq 0.31 mm/mm Hg, blue line and box) compared to those with RV–PA uncoupling (TAPSE/PASP ratio <0.31 mm/mm Hg, red line and box) during the follow-up after significant secondary TR diagnosis.

RV-PA = Right ventricular – pulmonary arterial; TAPSE/PASP = Tricuspid annular plane systolic excursion / pulmonary artery systolic pressure ratio; TR = Tricuspid regurgitation.

Table 3
Univariable and multivariable Cox proportional hazard models for all-cause mortality

	Univariate analysis		Multivariable analysis	
	HR (95% CI)	p value	HR (95% CI)	p value
Patient demographics and comorbidities				
Age	1.023 (1.015-1.030)	<0.001	1.030 (1.020-1.040)	<0.001
Men	1.199 (1.019-1.410)	0.029	1.135 (0.908-1.419)	0.267
Atrial fibrillation	0.992 (0.841-1.170)	0.922		
Current or former smoker	1.178 (0.985-1.409)	0.073		
Hypertension	0.956 (0.771-1.185)	0.681		
Diabetes mellitus	1.765 (1.454-2.143)	<0.001	1.294 (1.024-1.634)	0.031
Coronary artery disease	1.690 (1.436-1.989)	<0.001	1.229 (0.995-1.517)	0.055
Chronic obstructive pulmonary disease	1.641 (1.322-2.037)	<0.001	1.157 (0.902-1.484)	0.251
Estimated glomerular filtration rate	0.983 (0.980-0.987)	<0.001	0.992 (0.987-0.996)	<0.001
New York Heart Association III-IV	2.466 (2.077-2.927)	<0.001	1.774 (1.445-2.177)	<0.001
Diuretics	2.188 (1.826-2.563)	<0.001	1.328 (1.045-1.688)	0.020
Peripheral edema	1.768 (1.462-2.137)	<0.001	1.060 (0.839-1.338)	0.626
Echocardiographic parameters				
Left ventricular ejection fraction	0.984 (0.979-0.989)	<0.001	0.997 (0.990-1.004)	0.359
Left atrial maximum volume	1.002 (1.001-1.004)	0.001	1.000 (0.998-1.002)	0.748
Significant mitral regurgitation	1.473 (1.236-1.756)	<0.001	1.163 (0.941-1.437)	0.162
Significant aortic stenosis	1.454 (1.210-1.747)	<0.001	1.200 (0.967-1.489)	0.098
Tricuspid annulus diameter	1.014 (1.004-1.025)	0.006		
Right ventricular basal diameter	1.020 (1.011-1.030)	<0.001	1.008 (0.994-1.022)	0.259
Right ventricular base-to-apex length	1.015 (1.008-1.022)	<0.001	1.008 (0.998-1.018)	0.106
Right ventricular end-diastolic area	1.009 (1.006-1.013)	<0.001		
Fractional area change	0.198 (0.108-0.366)	<0.001		
TAPSE	0.940 (0.923-0.957)	<0.001		
Right atrial area	1.006 (1.000-1.013)	0.063		
PASP	1.022 (1.017-1.027)	<0.001		
Pace-maker/implantable cardioverter defibrillator lead	1.312 (1.112-1.548)	0.001	1.149 (0.938-1.409)	0.180
Vena contracta width	1.027 (1.006-1.048)	0.010	1.010 (0.985-1.035)	0.445
Regurgitant volume	1.002 (1.001-1.004)	0.001		
RV-PA uncoupling (TAPSE/PASP<0.31)	2.117 (1.799-2.492)	<0.001	1.462 (1.192-1.793)	<0.001

CI = confidence intervals; HR = hazard ratio; PA = pulmonary arterial; PASP = pulmonary artery systolic pressure; TAPSE = tricuspid annular plane systolic excursion.

It has been extensively demonstrated that RV systolic performance is closely related to afterload and should be evaluated together with the assessment of RV-PA coupling.^{8,9,13,14,16} The noninvasive assessment of RV-PA coupling with the TAPSE/PASP ratio has been shown to correlate well with invasive hemodynamics and more importantly, predict outcomes in several cardiovascular diseases, such as pulmonary arterial hypertension, heart failure with reduced ejection fraction, heart failure with preserved ejection fraction, and severe aortic stenosis.^{8,9,13,14,16} Although these cardiovascular pathologies may coexist with significant TR, the prognostic importance of RV-PA coupling has not been extensively examined in a cohort of patients with significant secondary TR. The relationship between TAPSE and PASP evaluates the adaptation of RV systolic function to afterload and the ability of the RV to generate pulmonary pressures. Optimal RV-PA coupling occurs when RV contractility (Ees) and afterload (Ea) are equal or the ratio between the 2 is above 1, as this minimizes energy expenditure and maximizes efficiency.^{7,13} The RV adapts initially to pressure overload through RV hypertrophy to increase RV contractility at the expense of an increase in RV filling pressures and diastolic dysfunction. However, with progressive RV-PA uncoupling (Ees/Ea ratio < 0.8 that approximately corresponds to TAPSE/

PASP ratio < 0.31 mm/mm Hg,⁸) the RV progressively dilates and RV systolic dysfunction occurs.^{8,13,14} In secondary TR, pressure overload is likely the primary determinant of RV-PA uncoupling. However, in contrast to heart failure, aortic stenosis and pulmonary arterial hypertension, volume overload due to significant TR can contribute to RV dilatation and dysfunction. Volume overload may result in increased wall tension¹⁷ leading to myocardial fibrosis and altered RV chamber geometry, directly contributing to impaired RV contractility and therefore, RV-PA uncoupling.^{7,18} From this perspective, RV-PA uncoupling represents a final common pathway of chronic RV pressure and volume overload in secondary TR.

In this large cohort of patients with moderate or severe secondary TR, 41% of the study population presented with a TAPSE/PASP ratio < 0.31 mm/mm Hg at the time of significant TR diagnosis, reflecting RV-PA uncoupling. Patients with RV-PA uncoupling showed a higher prevalence of heart failure symptoms and comorbidities, with more severe TR and advanced RV remodeling. This is in accordance with previous studies where a lower TAPSE/PASP ratio was related to advanced right heart remodeling, secondary TR, and impaired functional capacity.^{8,9,13,14} Importantly, after adjusting for known comorbidities, cardiovascular risk factors and several echocardiographic

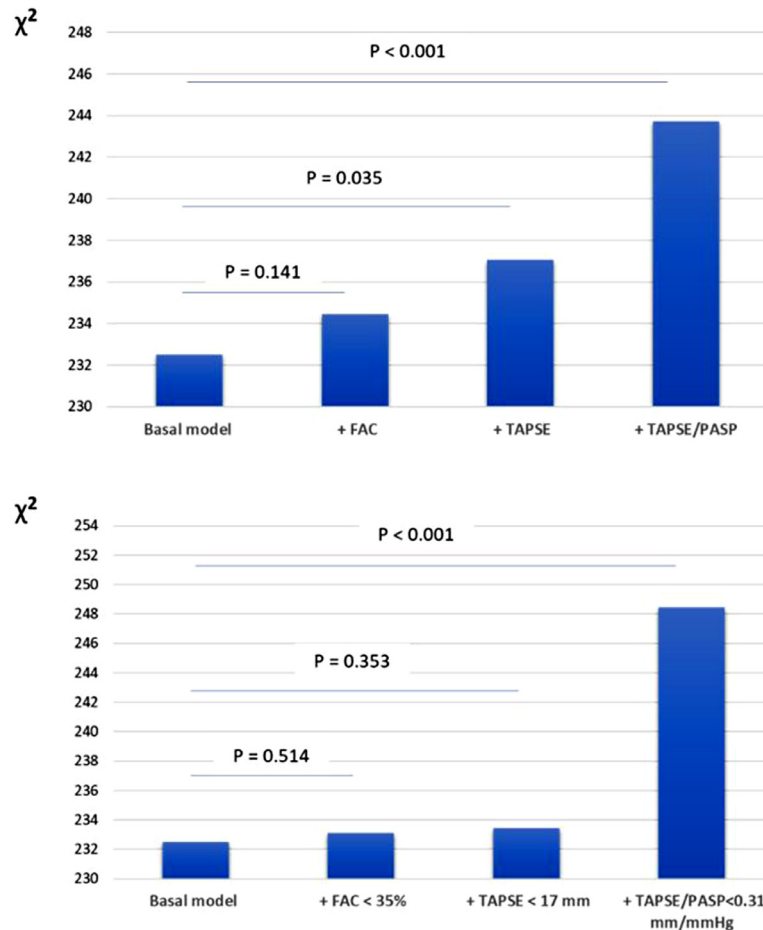


Figure 3. Incremental prognostic value of RV-PA uncoupling. The bar-graph in the upper panel shows a statistically significant increase in Chi-square with the addition of TAPSE/PASP as a continuous variable to a basal model (including age, gender, diabetes, known coronary artery disease, chronic obstructive pulmonary disease, estimated glomerular filtration rate, NYHA classes III and IV, diuretic use, peripheral edema, LVEF, LA volume, significant mitral regurgitation, significant aortic stenosis, RV basal diameter, RV base-to-apex length, presence of PM/ICD lead, tricuspid regurgitation VC width) compared to the addition of standard echocardiographic indices of RV systolic function (i.e., FAC or TAPSE). The bar-graph in the lower panel demonstrates a greater increase in chi-square with the addition of RV-PA uncoupling (i.e., TAPSE/PASP < 0.31 mm/mm Hg) to the basal model compared to the addition of RV systolic dysfunction either defined with FAC (<35%) or TAPSE (<17 mm).

FAC = Fractional area change; ICD = Implantable cardioverter defibrillator; LA = Left atrial; LVEF = Left Ventricular Ejection Fraction; NYHA = New York Heart Association; PM = Pace-maker; RV = Right ventricular; RV-PA = Right ventricular - pulmonary arterial; TAPSE/PASP = Tricuspid annular plane systolic excursion / pulmonary artery systolic pressure ratio; TR = Tricuspid regurgitation; VC = Vena contracta.

parameters, the noninvasive evaluation of RV-PA coupling (i.e., TAPSE/PASP ratio) was independently associated with prognosis and was incremental to the evaluation of conventional RV systolic function indices that do not take RV afterload into account. Interventions aimed at reducing RV pressure and volume overload could have a beneficial effect on RV systolic function and therefore improve RV-PA coupling and patient prognosis. In patients with heart failure due to reduced left ventricular systolic function and significant functional mitral regurgitation, sacubitril/valsartan showed to have a beneficial effect on left ventricular systolic and diastolic function and to reduce mitral regurgitation severity,¹⁹ potentially leading to a progressive decrease in pulmonary pressures and improved RV-PA coupling. Supplemental oxygen in patients with chronic obstructive pulmonary disease may reduce hypoxemia and pulmonary pressures, optimizing RV-PA coupling.²⁰ Finally, tricuspid valve interventions

can reduce RV volume overload,^{21,22} and therefore could have a beneficial effect on RV-PA coupling, potentially improving the prognosis of these patients. Although we showed that RV-PA uncoupling in patients with significant TR is independently associated with a worse prognosis if TR is left untreated, prospective studies potentially including also invasive hemodynamic data are warranted to provide further insights on the role of the non-invasive assessment of RV-PA coupling to improve patient selection for tricuspid valve interventions.²³

The limitations of the present study are inherent to its single-center retrospective design. Although echocardiography may underestimate pulmonary pressures in the presence of significant TR, the correction of RV systolic function for PASP significantly improved the predictivity of the Cox models compared to the independent use of conventional echocardiographic indices of RV systolic function. Despite the higher accuracy of invasive pressure

–volume loops to estimate RV–PA coupling, standard echocardiography provides a reliable measure of the adaptation of RV to the increased afterload,⁸ is widely available and allows for repetitive non-invasive assessment without any additional risk for patients. Finally, in the present study, RV–PA coupling was assessed only at rest, further studies would be needed to investigate the role of exercise echocardiography to unmask RV–PA uncoupling and risk-stratify patients with secondary TR.

In conclusion, the echocardiographic estimation of RV–PA coupling with the TAPSE/PASP ratio improves risk stratification of patients with significant secondary TR compared to the use of conventional echocardiographic indices of RV systolic function.

Authors' contributions

Federico Fortuni: Conceptualization; Data curation; Formal analysis; Investigation; Methodology; Project administration; Resources; Validation; Visualization; Writing—original draft. Steele C. Butcher: Conceptualization; Data curation; Formal analysis; Methodology; Project administration; Resources; Validation; Writing—original draft. Marlieke Dietz: Conceptualization; Data curation; Methodology; Resources; Validation; Writing—review & editing. Pieter van der Bijl: Conceptualization; Data curation; Methodology; Resources; Validation; Writing—review & editing. Edgard A. Prihadi: Data curation; Resources; Validation; Writing—review & editing. Gaetano De Ferrari: Writing—review & editing. Nina Ajmone Marsan: Conceptualization; Funding acquisition; Methodology; Project administration; Supervision; Validation; Writing—review & editing. Jeroen J. Bax: Conceptualization; Data curation; Funding acquisition; Methodology; Project administration; Resources; Supervision; Validation; Writing—review & editing. Victoria Delgado: Conceptualization; Data curation; Funding acquisition; Methodology; Project administration; Resources; Supervision; Validation; Writing—review & editing.

Disclosures

The Department of Cardiology of the Leiden University Medical Center received research grants from Abbott Vascular, Bayer, Bioventrix, Medtronic, Biotronik, Boston Scientific, GE Healthcare, and Edwards Lifesciences. Jeroen Bax and Nina Ajmone Marsan received speaking fees from Abbott Vascular. Victoria Delgado received speaker fees from Abbott Vascular, Medtronic, Edwards Lifesciences, MSD, Novartis and GE Healthcare. The remaining authors have nothing to disclose.

Supplementary materials

Supplementary material associated with this article can be found in the online version at <https://doi.org/10.1016/j.amjcard.2021.02.037>.

1. Nath J, Foster E, Heidenreich PA. Impact of tricuspid regurgitation on long-term survival. *J Am Coll Cardiol* 2004;43:405–409.

2. De la Espriella R, Santas E, Chorro FJ, Miñana G, Soler M, Bodí V, Valero E, Núñez E, Bayés-Genis A, Lupón J, Sanchis J, Núñez J. Functional tricuspid regurgitation and recurrent admissions in patients with acute heart failure. *Int J Cardiol* 2019;291:83–88.
3. Stuge O, Liddicoat J. Emerging opportunities for cardiac surgeons within structural heart disease. *J Thorac Cardiovasc Surg* 2006;132:1258–1261.
4. Arsalan M, Walther T, Smith RL, Grayburn PA. Tricuspid regurgitation diagnosis and treatment. *Eur Heart J* 2017;38:634–638.
5. Badano LP, Muraru D, Enriquez-Sarano M. Assessment of functional tricuspid regurgitation. *Eur Heart J* 2013;34:1875–1885.
6. Prihadi EA, Delgado V, Leon MB, Enriquez-Sarano M, Topilsky Y, Bax JJ. Morphologic types of tricuspid regurgitation: characteristics and prognostic implications. *JACC Cardiovasc Imaging* 2019;12:491–499.
7. Sanz J, Sanchez-Quintana D, Bossone E, Bogaard HJ, Naeije R. Anatomy, and dysfunction of the right ventricle: JACC state-of-the-art review. *J Am Coll Cardiol* 2019;73:1463–1482.
8. Tello K, Wan J, Dalmer A, Vanderpool R, Ghofrani HA, Naeije R, Roller F, Mohajerani E, Seeger W, Herberg U, Sommer N, Gall H, Richter MJ. Validation of the tricuspid annular plane systolic excursion/systolic pulmonary artery pressure ratio for the assessment of right ventricular-arterial coupling in severe pulmonary hypertension. *Circ Cardiovasc Imaging* 2019;12:e009047.
9. Tello K, Axmann J, Ghofrani HA, Naeije R, Narcin N, Rieth A, Seeger W, Gall H, Richter MJ. Relevance of the TAPSE/PASP ratio in pulmonary arterial hypertension. *Int J Cardiol* 2018;266:229–235.
10. Rudski LG, Lai WW, Afilalo J, Hua L, Handschumacher MD, Chandrasekaran K, Solomon SD, Louie EK, Schiller NB. Guidelines for the echocardiographic assessment of the right heart in adults: A report from the American Society of Echocardiography endorsed by the European Association of Echocardiography, a registered branch of the European Society of Cardiology, and the Canadian Society of Echocardiography. *J Am Soc Echocardiogr* 2010;23:685–713.
11. Zoghbi WA, Adams D, Bonow RO, Enriquez-Sarano M, Foster E, Grayburn PA, Hahn RT, Han Y, Hung J, Lang RM, Little SH, Shah DJ, Sherman S, Thavandiranathan P, Thomas JB, Weissman NJ. Recommendations for noninvasive evaluation of native valvular regurgitation: a report from the American Society of Echocardiography Developed in Collaboration with the Society for Cardiovascular Magnetic Resonance. *J Am Soc Echocardiogr* 2017;30:303–371.
12. Lang RM, Badano LP, Mor-Avi V, Afilalo J, Armstrong A, Ernande L, Flachskampf FA, Foster E, Goldstein SA, Kuznetsova T, Lancellotti P, Muraru D, Picard MH, Rietzschel ER, Rudski L, Spencer KT, Tsang W, Voigt JU. Recommendations for cardiac chamber quantification by echocardiography in adults: an update from the American Society of Echocardiography and the European Association of Cardiovascular Imaging. *J Am Soc Echocardiogr* 2015;28:1–39.e14.
13. Guazzi M, Bandera F, Pelissero G, Castelvecchio S, Menicanti L, Ghio S, Temporelli PL, Arena R. Tricuspid annular plane systolic excursion and pulmonary arterial systolic pressure relationship in heart failure: an index of right ventricular contractile function and prognosis. *Am J Physiol Heart Circ Physiol* 2013;305:H1373–H1381.
14. Guazzi M, Dixon D, Labate V, Beussink-Nelson L, Bandera F, Cuttica MJ, Shah SJ. RV contractile function and its coupling to pulmonary circulation in heart failure with preserved ejection fraction: stratification of clinical phenotypes and outcomes. *JACC Cardiovasc Imaging* 2017;10:1211–1221.
15. Galderisi M, Cosyns B, Edvardsen T, Cardim N, Delgado V, Di Salvo G, Donal E, Sade LE, Ernande L, Garbi M, Grapsa J, Hagendorff A, Kamp O, Magne J, Santoro C, Stefanidis A, Lancellotti P, Popescu B, Habib G, 2016–2018 EACVI Scientific Documents Committee. Standardization of adult transthoracic echocardiography reporting in agreement with recent chamber quantification, diastolic function, and heart valve disease recommendations: an expert consensus document of the European Association of Cardiovascular Imaging. *Eur Heart J Cardiovasc Imaging* 2017;18:1301–1310.
16. Tadic M, Pieske-Kraigher E, Cuspidi C, Morris DA, Burkhardt F, Baudisch A, Hafeld S, Tschöpe C, Pieske B. Right ventricular strain in heart failure: clinical perspective. *Arch Cardiovasc Dis* 2017;110:562–571.
17. Fortuni F, Dietz MF, Butcher SC, Prihadi EA, van der Bijl P, Ajmone Marsan N, Delgado V, Bax JJ. Prognostic implications of increased

- right ventricular wall tension in secondary tricuspid regurgitation. *Am J Cardiol* 2020;136:131–139.
18. Bossone E, D'Andrea A, D'Alto M, Citro R, Argiento P, Ferrara F, Cittadini A, Rubenfire M, Naeije R. Echocardiography in pulmonary arterial hypertension: from diagnosis to prognosis. *J Am Soc Echocardiogr* 2013;26:1–14.
 19. Kang DH, Park SJ, Shin SH, Hong GR, Lee S, Kim MS, Yun SC, Song JM, Park SW, Kim JJ. Angiotensin receptor neprilysin inhibitor for functional mitral regurgitation. *Circulation* 2019;139:1354–1365.
 20. Stoller JK, Panos RJ, Krachman S, Doherty DE, Make B, Long-term Oxygen Treatment Trial Research Group. Oxygen therapy for patients with COPD: current evidence and the long-term oxygen treatment trial. *Chest* 2010;138:179–187.
 21. Karam N, Mehr M, Taramasso M, Besler C, Ruf T, Connelly KA, Weber M, Yzeiraj E, Schiavi D, Mangieri A, Vaskelyte L, Alessandrini H, Deuschl F, Brugger N, Ahmad H, Ho E, Biasco L, Orban M, Deseive S, Braun D, Gavazzoni M, Rommel KP, Pozzoli A, Frerker C, Nábauer M, Massberg S, Pedrazzini G, Tang GHL, Windecker S, Schäfer U, Kuck KH, Sievert H, Denti P, Latib A, Schofer J, Nickenig G, Fam N, von Bardeleben S, Lurz P, Maisano F, Hausleiter J. Value of echocardiographic right ventricular and pulmonary pressure assessment in predicting transcatheter tricuspid repair outcome. *JACC Cardiovasc Interv* 2020;13:1251–1261.
 22. Hahn RT, Meduri CU, Davidson CJ, Lim S, Nazif TM, Ricciardi MJ, Rajagopal V, Ailawadi G, Vannan MA, Thomas JD, Fowler D, Rich S, Martin R, Ong G, Groothuis A, Kodali S. Early feasibility study of a transcatheter tricuspid valve annuloplasty: SCOUT trial 30-day results. *J Am Coll Cardiol* 2017;69:1795–1806.
 23. D'Alto M, Naeije R. Transcatheter tricuspid valve repair in patients with pulmonary hypertension. *Eur Heart J* 2020;41:2811–2812.